Current Simulation of a Controlled PMSM including Skew and Torsional Rotor Vibrations

M. Jaeger, S. Rick, K. Hameyer

***Abstract* – For the simulation of permanent magnet synchronous machines many models at different levels of complexity are described in literature. In basic cases, the common equations lead to good and quick results, but do omit nonlinear and transient effects such as slotting, saturation, rotor movement and production deviations. In this paper, a transient model based on look-up table data from non-linear finite element analysis (FEA) is applied to a traction drive motor and extended to represent multiple rotor slices. The FEA is done in advance in parallel leading to a fast transient model. The derivation of the machine equations for multiple slices and the model are presented. Simulated currents are validated with measurement. Following the model is used to show the impact of different influence factors like skew, rotor torsion and pulse width modulation (PWM).**

***Index Terms* — Permanent Magnet Synchronous Machines, Rotor Vibration, Controlled PMSM**

I. Introduction

The increasingly fast growing sector of electric vehicles has led to new demands for electrical traction drives. The permanent magnet excited synchronous machine (PMSM) is a common choice of machine type in these applications due to the high efficiency and power density. Additional to the pure performance in the automotive sector sound and feel are important unique selling points of a vehicle. In the past, the main goal of acoustic machine design usually was the reduction of noise and vibrations rather than designing a specific sound characteristic. To fulfill such requirements of a highly dynamic traction motor driven by PWM in modern vehicles and other applications a deeper understanding of the nonlinear multi-physical dependencies of the electrical machine is necessary.

To improve and design the machine acoustics the use of a continuous or stepped skew in rotor or stator to reduce torque ripple, cogging torque, back EMF harmonics and acoustic performance is a common technique and extensively studied [1][2]. However, many papers focus solely on torque ripple and/or back EMF [3][4], also primarily regarding the open circuit (no load) performance, which in general can be improved and described by a skewing factor [5]. In [6] it was found that the torque ripple at full load is significantly higher than at no load, while in [1] and [7] small PMSMs were studied where skewing decreased the torque ripple at no load while increasing it at full load.

The effective angle between rotor and stator field over the axial machine length is additionally influenced by rotor torsion due to load and torsional oscillations. A high constructional freedom of rotor and shaft is desirable to incorporate cooling solutions [8] or due to application requirements [9]. A hollow or otherwise uncommon rotor however usually has a lower stiffness significantly lowering the torsional eigenfrequencies and increasing oscillation amplitudes. Furthermore, for specific cases torsional vibrations occur in a strength which has to be considered [10][11]. The retroactive effects between the mechanical domain including torsional oscillations of skewed rotors and the electromagnetic behavior including controller and power electronics are rarely studied.

In [12] and [13] a system model for the simulation of a controlled PMSM is developed featuring a strong coupling between mechanical and electromagnetic domain. The approach of mapping machine parameters in advance in Look Up Tables (LUTs) offers the possibility to split the computational effort via parallelization in comparison to approaches such as circuit coupled iterative FEA. The approach includes slotting effects, cross coupling and saturation, which is relevant for a successful distinction between the said effects and the influence of torsion and skew.

While the model from [12] and [13] shows good results in these papers, it lacks the ability to describe skew and torsional rotor vibrations. Therefor in this paper the model is extended to the description of stepped and continuous skew and torsion by the multislice method from [14][15] featuring a variable slice count. This allows determination of the influence of skew and torsional vibrations on the current via relatively quick simulations. Additionally the relation between rotor discretization (meaning slice count) and accuracy of results can be obtained, and the model from [12][13] is further validated by application to a small traction drive motor. Simulation results in comparison to measurement and the influence of skew and torsion is shown before the paper is concluded.

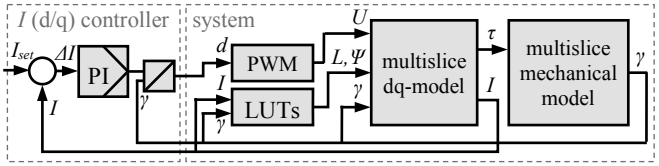

Fig. 1 Overview of the model structure with the forward feed of voltage and the strongly coupled feedback via current and machine angle.

M.Jaeger is with the Institute of Electrical Machines, RWTH University, Aachen, GER, (email: markus.jaeger@iem.rwth-aachen.de).

S.Rick contributes as former member of the Institute of Electrical Machines, RWTH University, Aachen, GER, (email: sebastian.rick@iem.rwth-aachen.de).

K. Hameyer is with the Institute of Electrical Machines, RWTH Aachen University, Aachen, GER (email: kay.hameyer@iem.rwth-aachen.de)

This work was performed as part of the research training group GRK 1856 by the Deutsche Forschungsgemeinschaft (DFG) in cooperation with the projects No. 682 I and 682 II organized by the Forschungsvereinigung Antriebstechnik e.V. (FVA) in Germany and funded by AiF in the frame work of the program of Industrielle Gemeinschaftsforschung (IGF) by the Federal Ministry for Economic Affairs and Energy (BMWi).

II. DQ-Model including Multislice Method

The utilized model is illustrated in Fig 1. It is derived from the basic equations of a synchronous machine in the rotor aligned two axis dq-coordinate system which link the machine voltages U and currents I depending on the machine state described by the time dependent magnitudes rotational angle γ, flux Ψ and inductances L. The forward path of the loop incorporates at the first stage the current controller which supplies the set point for voltage as duty cycle d to the power electronics, which again reproduces the sinusoidal voltages of the 3-phase coordinate system by PWM. In combination with the variable machine state parameters from the LUTs the machine equations are used to compute the curents at each timestep. The torque τ extracted from the FEA corresponding to the calculated current is fed into a mechanical model of torsinal spring-damper-elements of the rotor and drivetrain.

For basic considerations, which do not account for skew and torsion, the average rotor position leads to reasonable accurate results, especially if the focus is not acoustics and regarding other relevant effects like slotting, saturation, harmonics due to PWM or controller influence that can dominate the effects of skew and torsion.

The approach of this paper is based on the multislice method whose principle is illustrated in Fig 2. In axial direction the machine is regarded as a series of n slices without skew and therefore constant angle between rotor and stator field. The advantage is the possibility to use 2D-FEA to describe the machine state in each slice over more complex and computationally extensive 3D Simulations. For a continuously skewed machine this leads to a discretization error, while for stepwise skewed machines the only error comes from the neglected effects in axial direction between slices of different angle.

The starting point of the extended multislice model is the general equation for the voltage u of a synchronous machine with the time dependent current $i(t)$, ohmic resistances R and the flux linkage ψ

$$u = R \cdot i(t) + \frac{d}{dt}\psi. \tag{1}$$

The flux linkage can be divided in a part resulting from the permanent magnet excitation ψ_f and a part based on the currents ψ_i and the machine inductances L

$$\psi = \psi_f + \psi_i = \psi_f + L \cdot i(t) \tag{2}$$

which leads to the following equation (3) linking the voltage with the machine currents

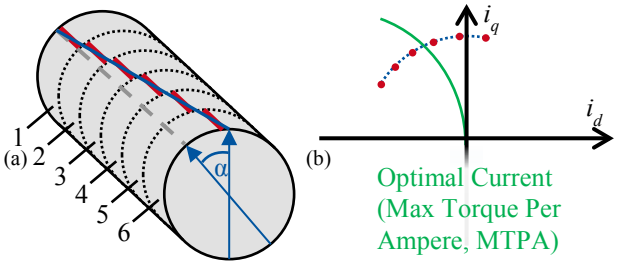

Fig. 2 (a) Illustration of the multislice method at the example of a continuously skewed rotor with skew angle α approximated by six slices. (b) Location of the slices field in the rotor-aligned dq-coordinate system.

$$u = R \cdot i(t) + \frac{d}{dt}[\psi_f + L \cdot i(t)]. \tag{3}$$

So far no assumptions where made limiting the validity. The common idealized model of a synchronous machine neglects saturation and slotting effects considering only the fundamental wave, resulting in fixed values for the flux linkage and inductance matrices. Saturation leads to a nonlinear dependency of flux linkage and inductances to the machine current, whereas slotting is a dependency of the rotor position, which for an ideal machine is given by its angle γ.

$$\psi = \psi(i,\gamma) \quad resp. \quad L = L(i,\gamma) \tag{4}$$

This leads to the rotor position and current state depending voltage equation for the synchronous machine (5):

$$u = R \cdot i(t) + \frac{d}{dt}[\psi_f(i(t),\gamma) + L(i(t),\gamma) \cdot i(t)]. \tag{5}$$

To calculate the machine currents from the supply voltage the voltage equation has to be solved for the current. For practicability, and due to the fact that the regarded machine is a permanent magnet synchronous machine, this is done in the rotor-aligned dq-system:

$$u_d = R_{dd} i_d + \frac{d}{dt}[\psi_{fd}(i_d, i_q, \gamma) + L_{dd}(i_d, i_q, \gamma) \cdot i_d + L_{dq}(i_d, i_q, \gamma) \cdot i_q] \tag{6a}$$

$$u_q = R_{qq} i_q + \frac{d}{dt}[\psi_{fq}(i_d, i_q, \gamma) + L_{dq}(i_d, i_q, \gamma) \cdot i_d + L_{qq}(i_d, i_q, \gamma) \cdot i_q]. \tag{6b}$$

The self-inductances L_{dd}, L_{qq} and the mutual inductance L_{dq} (equal to L_{qd}) are elements of the inductance matrix, analogously the elements of the resistance matrix with the difference that R_{dq} and R_{qd} have to be zero. Execution of the time derivative and restructuring leads to

$$u_d = \frac{di_d}{dt} \cdot A + \frac{di_q}{dt} \cdot B + X \tag{7a}$$

$$u_q = \frac{di_d}{dt} \cdot C + \frac{di_q}{dt} \cdot D + Y \tag{7b}$$

with the following abbreviations which only depend on the mapped parameters describing the machine state

$$A = L_{dd} + \frac{d\psi_{fd}}{di_d} + \frac{dL_{dd}}{di_d} \cdot i_d + \frac{dL_{dq}}{di_d} \cdot i_q \tag{8a}$$

$$B = L_{dq} + \frac{d\psi_{fd}}{di_q} + \frac{dL_{dd}}{di_q} \cdot i_d + \frac{dL_{dq}}{di_q} \cdot i_q \tag{8b}$$

$$C = L_{dq} + \frac{d\psi_{fq}}{di_d} + \frac{dL_{dq}}{di_d} \cdot i_d + \frac{dL_{qq}}{di_d} \cdot i_q \tag{8c}$$

$$D = L_{qq} + \frac{d\psi_{fq}}{di_q} + \frac{dL_{dq}}{di_q} \cdot i_d + \frac{dL_{qq}}{di_q} \cdot i_q \tag{8d}$$

$$X = \omega\left(\frac{d\psi_{fd}}{d\gamma} - \psi_{fq} + i_d\left(\frac{dL_{dd}}{d\gamma} - L_{dq}\right) - i_q\left(\frac{dL_{dq}}{d\gamma} - L_{qq}\right)\right) + R_{dd} \cdot i_d \tag{8e}$$

$$Y = \omega\left(\frac{d\psi_{fq}}{d\gamma} - \psi_{fd} + i_d\left(\frac{dL_{dq}}{d\gamma} + L_{dd}\right) + i_q\left(\frac{dL_{qq}}{d\gamma} + L_{dq}\right)\right) + R_{qq} \cdot i_q \tag{8e}$$

In tensor notation the restructured machine equations (7a..b) with the abbreviations (8a..e) can be written as

$$u = \begin{bmatrix} A & B \\ C & D \end{bmatrix} \cdot \frac{di}{dt} + \begin{pmatrix} X \\ Y \end{pmatrix} = M \frac{di}{dt} + N \tag{9}$$

Equation (9) has to be solved for each slice with the machine state parameters (flux and inductances) of that slice which depend on the angular position of the slice and the dq-current in the slices dq-coordinate system.

The supplied voltage u drops over the series of all n slices, while the change in current di/dt is the same at every slice for a common coordinate system. Furthermore, the angle difference θ_j between rotor and stator field for each slice has to be taken into account via a rotation matrix $Rot(\theta_j)$, leading to the following voltage equation (10) for n slices:

$$u = \sum_j^n u_j = \sum_j^n Rot(\theta_j)\left(M_j \cdot \frac{di}{dt} + N_j\right) \tag{10}$$

$$\text{with} \qquad Rot(\theta_j) = \begin{bmatrix} \cos(\theta_j) & -\sin(\theta_j) \\ \sin(\theta_j) & \cos(\theta_j) \end{bmatrix} \tag{10a}$$

The final step is solving for the current derivative:

$$\frac{di}{dt} = \left[\sum_j^n \left(Rot(\theta_j) M_j Rot(\theta_j)^{-1}\right)\right]^{-1} \cdot \left[u - \sum_j^n \left(Rot(\theta_j)\right)\right] \tag{11}$$

III. Determination of the Machine Parameters

The necessary magnitudes describing the machine state are gathered in advance by Finite Element Analysis (FEA) based on the assumption of a quasi-static flux solution without eddy currents or hysteresis losses. The neglection of eddy currents is feasible due to the buried permanent magnets of the regarded machine. The alternating stator field has a low penetration depth on the rotor iron and therefor does not reach the not laminated permanent magnets. The assumption of no hysteresis leads to overestimated flux and magnetomotive forces at high frequencies where the hysteresis loop of the soft magnetic materials widens significantly.

A. Flux Linkage

The total machine flux in any operating point is computed from the vector potential as solution of the FEA. The excitation flux, hence the part resulting from the permanent magnets, can then be computed by solving the system again with only magnet excitation and zero current while holding the saturation state constant.

B. Inductances

The machine inductances are derived by the method described in [16]. The principle is related to the computation of the excitation flux: At first, the finite element problem is solved for one operating point. Subsequently the winding currents are changed one after another and the system solved again linearly with a fixed saturation state. From the change in flux in respect to the current the inductances are determined.

C. Discretization

The operating points, which have to be simulated with the FEA, are given by the dimensions current i_d, current i_q and rotational angle γ.

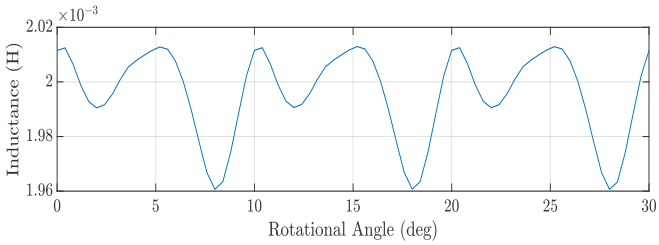

Fig. 3 Inductance L_{dd} over rotation of one pole for a fixed dq-current.

Discretization of the dimensions has a great impact on the number of FEAs necessary. For the regarded PMSM with six pole pairs and 36 teeth a stepping of 0.4° mechanical angle and 20 A (from -300A to 300 A effective current) are chosen as a compromise between accuracy and computational effort. In fig. 3 the value of the self-inductance of the d-axis is shown to illustrate this decision. Although reasonably smooth, some unsteadiness is visible, in particular at the minima. Since skew, torsion, a load step and other factors can lead to short time displacements of the dq-current, it is not sufficient to simulate only the near optimal area in the dq-plane.

To reduce the number of FE computations only one half (positive or negative current) of the q-axis can be simulated since the other half is symmetric/antisymmetric and therefor can be computed via mirroring. It should be stated that some production deviations, i.e. rotor eccentricity, break this symmetry.

The excitation flux of the direct axis for all current combinations, averaged over the rotational angle, is shown in fig. 4. The step width of 20 A is sufficient to map the d-excitation flux without aliasing artifacts.

More critical regarding discontinuities are the derivatives of inductances and fluxes. Exemplary in fig. 5 the derivative of the excitation flux ψ_{fd} with respect to the rotational angle γ is shown (at the arbitrary rotor position 1). It can be observed that at this rotor position at some current combinations (in case of this example at high positive d currents) variation between two points of the map is large compared to the overall variation. This limits the possible discretization stepwidth in the current and rotational angle direction in order to avoid ailasing artifacts which decrease the accuracy of the simulation results.

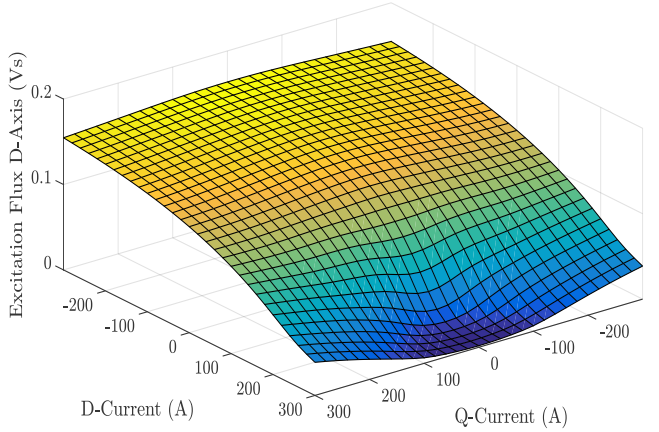

Fig. 4 Excitation flux ψ_{fd} over the current in d- and q-direction, averaged for all rotor positions.

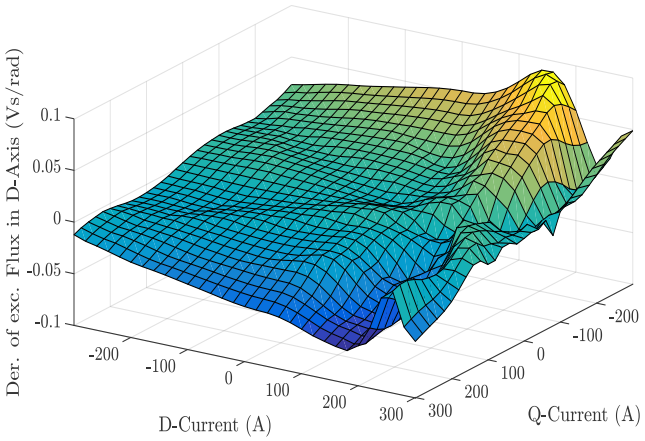

Fig. 5 Derivative of the excitation flux ψ_{fd} with respect to the rotational angle γ, at the first rotational position.

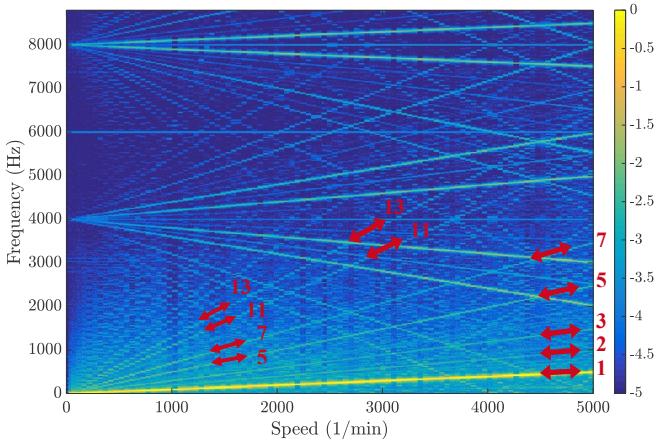

Fig. 6 Campbell-Diagram of one phase current from a measured stepwise run-up from 0 to 5000 RPM at medium load. Logarithmic scale relative to fundamental wave.

IV. Results

To validate the simulation, a 36-slot, 12-pole machine with a continuous skew of 9° was measured. The comparison for a run-up of the machine from 0 to 5000 RPM shows a good accordance between simulation and measurement (fig. 6, 7).

The fundamental wave (order 1) is clearly visible at the bottom of the logarithmic plot with the next highest harmonic being about factor $10^{-1.5}$ less. Due to the lack of uncertainties from the measurement and production deviations (geometric shape, anisotropic material behavior, varying permanent magnet remanence, etc.) the simulation in general displays a lot more distinguishable higher harmonics, which merge into each other in the Campbell diagram of the measurement. For a healthy machine harmonics of the orders 5, 7, 11, 13 (and an infinite number of higher order harmonics with decreasing amplitude) are expected. These orders are visible in both measurement and simulation, especially at lower frequencies, as marked in fig. 6 and fig. 7. The main harmonics of the PWM at double the PWM frequency of 4 kHz are also visible, as well as a broad range of PWM harmonics originating from 4 kHz and 8 kHz (at zero speed).

In the simulation (fig. 7) the even machine harmonics of order 2, 4, 8 and 10 do exist, of which only order 2 can be found in the measurement. The most likely explanation for this are non-ideal effects like dynamic eccentricity and magnetization deviations, which the model does not take into account. In addition, the ideal IGBTs (perfect switches) as opposed to real IGBTs with finite current and voltage rise and fall times can lead to some differences. In section IV. C it is shown that the PWM is the main origin of current harmonics. Additional to the results presented in section IV. C simulations with different PWM frequencies show significantly different harmonic orders present. This indicates that the current is very sensible to changes of power electronics parameters. However, in the measurement (fig. 6) and the simulation (fig. 7) the same PWM frequency was used, which suggests that other power electronics parameters not present in the model do influence the current harmonics.

In the spectrogram of the measurement order 3 is visible which cancels out in case of an ideal machine, which can be easily derived from basic analytical equations. This indicates one or more types of production deviations in the measured

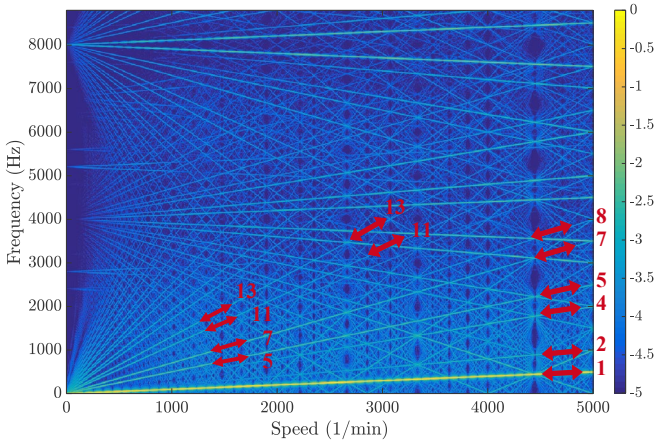

Fig. 7 Campbell-Diagram of one phase current from simulation of a continuous run-up from 0 to 5000 RPM at medium load with six slices. Logarithmic scale relative to fundamental wave.

machine like static/dynamic eccentricity. Further studies are necessary for an identification and separation.

A. *Skew*

To analyze the influence of skew in detail and to quantify the discretization error due to the multislice approach simulations with different amounts of slices have been carried out. Fig. 8 shows fourier transforms of one phase current at a constant speed of 625 RPM equal to 62.5 Hz fundamental frequency. In fig. 8 (a) the measurement is shown, (b) is the simulation without skew, (c) with 6 rotor slices and (d) with 18 rotor slices. In the case of a constant operating point the skew has a minor impact on current harmonics. Compared to the simulation without skew (b) the 6-slice case (c) shows a slight difference of the harmonic amplitudes. The 5th harmonic increases slightly while the 7th decreases, meaning a better accordance with the measurement where the 7th orders amplitude is only about 50% of the 5th. This deviation in amplitude is also assumed to result from production deviations. The amplitude of the direct PWM-induced frequencies at 8 kHz also slightly decreases, which are considerably lower in the measurement. To difference between the 6-slice simulation (c) and the 18-slice simulation (d) are barely noticeable but do lead to a significant slower execution due to the higher computational effort for 18 slices.

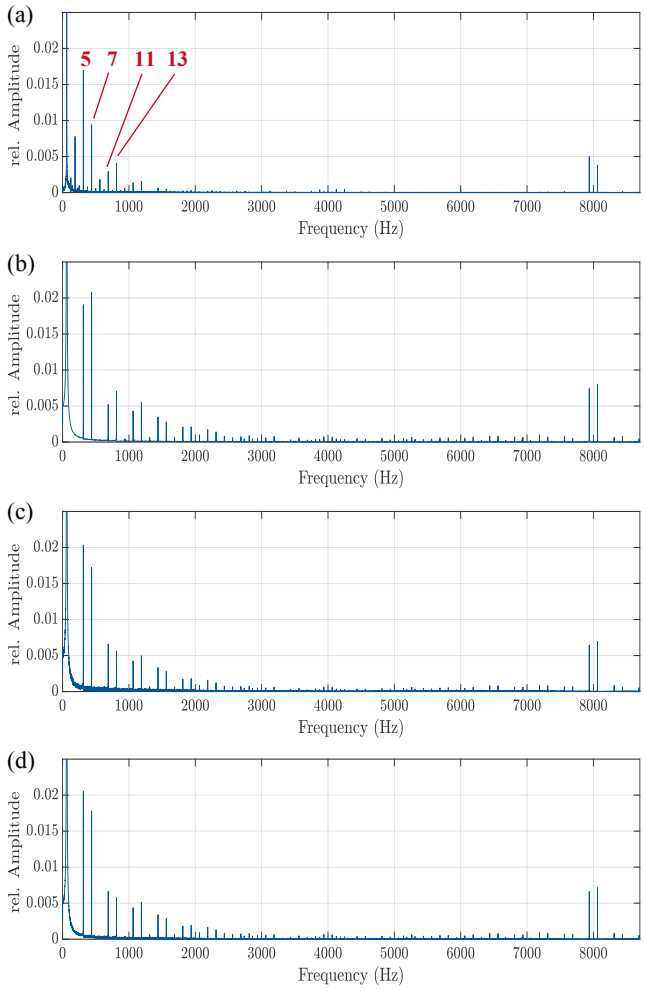

Fig. 8 Fourier transform of one phase current at a fundamental frequency of 62.5 Hz resp. 625 RPM. a) Measurement. b) Simulation without multislice. c) Six slices. d) 18 slices.

B. Torsional Vibrations

To study the effect of torsional rotor vibrations a simulative comparison between a rigid rotor and a torsional non-stiff rotor is performed. The mechanical model is adjusted to a torsional spring system with six slices of 20mm axial length representing a hollow shaft rotor construction. On one side of the shaft an inert mass represents a load attached via another torsional spring. A simulated run-up over 30 seconds from 0 to 5000 RPM shows multiple torsional rotor eigenmodes whose eigenfrequencies depend on the masses and torsional stiffness. Compared to a rigid rotor these oscillations led to additional harmonics in the current. This can be observed in fig. 9 of the rigid rotor run-up in comparison with fig. 10, where the additional harmonics are marked. The harmonics have a base frequency of 2 kHz indicating a connection to the PWM of 4 kHz.

C. Influence of PWM and controller

The model allows in-depth analysis of different influencing parameters which cannot be directly tested in practice. The obtained results of the skew and torsion influence show a minor direct dependency, while in case of torsional vibrations fractions of the PWM frequency occur as current harmonics. To determine the general impact of the PWM and controller frequency the results of additional simulations are shown in

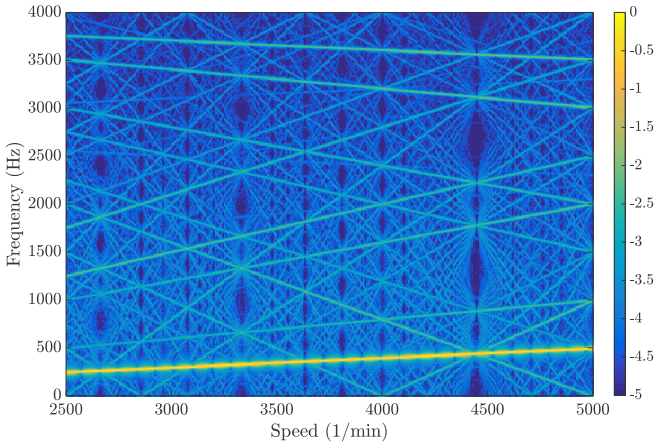

Fig. 9 Campbell-Diagram of one phase current from simulation of a continuous run-up from 0 to 5000 RPM at medium load with six slices. Logarithmic scale relative to fundamental wave. Rigid rotor.

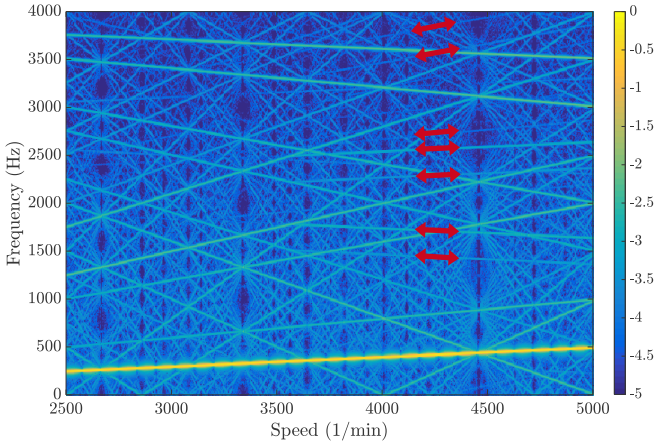

Fig. 10 Campbell-Diagram of one phase current from simulation of a continuous run-up from 0 to 5000 RPM at medium load with six slices. Logarithmic scale relative to fundamental wave. Torsional soft rotor showing oscillations leading to marked current harmonics.

fig. 11 and fig. 12. For fig. 11 the power electronics is bypassed, effectively allowing the controller to directly set voltages to the electrical machine model without time delay. This leads to a great decrease of harmonics as the controller is able to nearly ideally maintain the dq-currents constant. Only the lowest machine harmonic orders are observable with low amplitude, which eventually with adjusted controller settings could be completely reduced to zero. This simulative experiment proves that the primary origin of current harmonics is the power electronic with the PWM.

Since the set point voltages for the PWM result from the controller, the dependency between controller clock (the frequency at which new target voltages are computed) and current harmonics is examined. In fig. 12 different current harmonics are shown for different controller clock speeds at a fixed operating point at 4424 RPM. The PWM frequency was kept constant at 4 kHz. Fig. 12 (a) shows the result for a controller clock of 4 kHz. For ideal dead time compensation there are only minimal changes if multiples of the PWM frequency are used. Fig. 12 (b) shows results for a controller clock of 6 kHz as 3/2 of the PWM frequency and (c) for the odd number of 11 kHz. While the main machine harmonics (5,7,11,13) are still visible as well as the directly PWM

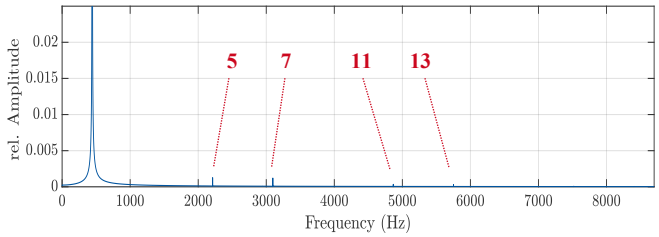

Fig. 11 Fourier transform of one phase current at a fundamental frequency of 442.4 Hz. Directly controlled machine without PWM.

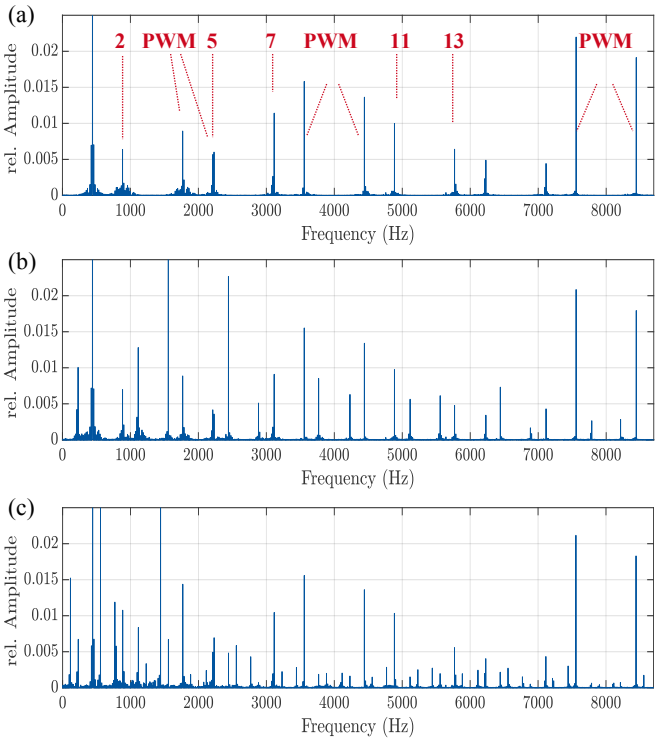

Fig. 12 Fourier transform of one phase current at a fundamental frequency of 442.4 Hz resp. 4424 RPM with PWM frequency at 4 kHz.
(a) Controller clock at 4 kHz. (b) Controller clock at 6 kHz.
(c) Controller clock at 11 kHz.

induced harmonics below and above 4 kHz a great number of additional harmonics can be observed. Matching the controller frequency to a multiple of the PWM frequency can greatly reduce the current harmonics.

V. Conclusion

In this paper a two-axis machine model of a PMSM capable of describing saturation, cross-coupling and slotting effects is studied and extended to support the multislice method as approximation of skewing and rotor torsion. The mathematical basis is presented and the model applied on a small traction drive. The method of parameter extraction from the FEA is presented in with regard to possible discretization errors. Validation of the model is performed comparing the fourier transformed phase currents to measurements from the machine which shows good accordance as the main harmonics are represented in the model. From differences in occurring harmonics between simulation of ideal machine and measurement a production deviation like eccentricity can be concluded, which makes an extension of the model to represent different production deviations seem promising. The model is further used to show the impact of skew and torsional vibrations. The representation of skew via multiple slices leads to a minor improvement of current harmonics compared to measurement, while torsional oscillations cause additional harmonics related to the PWM frequency. Additional simulations with the proposed model show a dominant dependency between PWM, controller frequency and phase current harmonics.

With the proposed model relatively fast repeated simulations are possible allowing a broad spectrum of different analyses regarding phase current, torque and force harmonics of machines with skew and torsional non-stiff rotor for a deeper understanding of acoustic machine behavior.

VI. References

[1] W. Q. Chu, Z. Q. Zhu, "Investigation of Torque Ripples in Permanent Magnet Synchronous Machines With Skewing," *IEEE Transactions on Magnetics*, vol. 47,iIssue 5, pp. 938-941, May 2011

[2] M. S. Islam, S. Mir, T. Sebastian, S. Underwood, "Design considerations of sinusoidally excited permanent-magnet machines for low-torque-ripple applications", *IEEE Transactions on Industry Applications*, vol. 41, no. 4, pp. 955-962, Jul.-Aug. 2005.

[3] S. Lee, Y.-J. Kim, S.-Y. Jung, "Numerical investigation on torque harmonics reduction of interior PM synchronous motor with concentrated winding", *IEEE Transactions on Magnetics*, vol. 48, no. 2, pp. 927-930, Feb. 2012.

[4] Z. Q. Zhu, D. Howe, "Influence of design parameters on cogging torque in permanent magnet machines", *IEEE Transactions on Energy Conversion*, vol. 15, no. 4, pp. 407-412, Dec. 2000.

[5] J. Pyrhonen, T. Jokinen, V. Hrabovcova, *Design of Rotating Electrical Machines*, U.K., Chichester:Wiley, 2008.

[6] H. S. Chen, D. G. Dorrell, M. C. Tsai, "Design and operation of interior permanent-magnet motors with two axial segments and high rotor saliency", *IEEE Transactions on Magnetics*, vol. 46, no. 9, pp. 3664-3675, Sep. 2010.

[7] Z. Azar, Z. Q. Zhu, G. Ombach, "Influence of electric loading and magnetic saturation on cogging torque back-EMF and torque ripple of PM machines", *IEEE Transactions on Magnetics*., vol. 48, no. 10, pp. 2650-2658, Oct. 2012.

[8] C. Nagpal; C. K. Jain, V. V. K. Reddy, "Rotor vent hole shape studies on totally enclosed fan cooled motor", *Power Electronics, Drives and Energy Systems (PEDES)*, Dec. 2012

[9] B. Janjic, A. Binder, V. Bischoff, G. Ludwig, "Design of PM integrated motor-drive system for axial pumps", *12 European Conf. on Power Electronics and Applications (EPE)*, Aalborg, Denmark, Sept. 2007.

[10] S. F. Rabbi ; M. A. Rahman , "Detection of torsional oscillations in line-start IPM motor drives using motor current signature analysis", *Electrical and Computer Engineering (ICECE)*, Dec. 2016

[11] V. Atarod, P. L. Dandeno, M. R. Iravani , "Impact of synchronous machine constants and models on the analysis of torsional dynamics", *IEEE Transactions on Power Systems, vol.* 7, issue 4, pp. 1456-1463, Nov 1992

[12] T. Herold, E. Lange, K. Hameyer, "System Simulation of a PMSM Servo Drive Using Field-Circuit Coupling," *IEEE Transactions on Magnetics*, vol. 47, issue 5, pp. 938-941, May 2011

[13] T. Herold, D. Franck, E. Lange, K. Hameyer, "Extension of a D-Q Model of a Permanent Magnet Excited Synchronous Machine by Including Saturation, Cross-Coupling and Slotting Effects," *Electric Machines & Drives Conference (IEMDC), 2011 IEEE International*, Mai 2011.

[14] Francis Piriou, Adel Razek, "A model for coupled magnetic-electric circuits in electric machines with skewed slots," *IEEE Transactions. on Magnetics*, vol. 26, no. 2, pp.1096-1 100, March, 1990.

[15] S. Williamson, T. J. Flack, A. F. Volschenk, "Representation of skew in time-stepped two-dimensional finite-element models of electrical machines", *IEEE Industry Applications. Society Annual Meeting*, Oct. 1994

[16] E. Lange, M. van der Giet, F. Henrotte, and K. Hameyer, "Circuit coupled simulation of a claw-pole alternator by a temporary linearization of the 3d-fe model", *Electrical Machines, 2008. ICEM 2008. 18th International Conference on*, pp. 1-6., Sept. 2008

VII. BIOGRAPHIES

Markus Jaeger received his M.Sc. degree in mechanical engineering from RWTH Aachen University, Aachen, Germany, in February 2016. He has been working as a research associate at the Institute of Electrical Machines of RWTH Aachen University, Germany since November 2016. His research interests include simulation and acoustical design of electrical machines as well as the vibrostrucutral behaviour of laminated stacks.

Sebastian Rick received his Dipl-Ing. degree in electrical engineering from RWTH Aachen University, Aachen, Germany, in May 2012. He has been working as a research associate at the Institute of Electrical Machines of RWTH Aachen University, Germany since June 2012. His research interests include new arts of electrical machines, simulation and acoustical design of electrical machines.

Kay Hameyer (M96-SM99) received the M.Sc. degree in electrical engineering from the University of Hannover, Germany, and the Ph.D. degree from the University of Technology Berlin, Germany. After his university studies he was with Robert Bosch GmbH, Stuttgart, Germany, as a Design Engineer for permanent-magnet servo motors and electrical board net components for vehicles. From 1996 to February 2004, he was a Full Professor of numerical field computations and electrical machines at the Katholieke Universiteit Leuven, Belgium. Since 2004 he is a Full Professor, the Director of the Institute of Electrical Machines, and the holder of the Chair Electromagnetic Energy Conversion at RWTH Aachen University, Aachen, Germany, where he has been the Dean of the Faculty of Electrical Engineering and Information Technology from 2007 to 2009. His research interests include numerical field computation and simulation, design of electrical machines, particularly permanent-magnet excited machines and induction machines, and numerical optimization strategies.